



ELSEVIER

Materials Characterization 48 (2002) 305–314

MATERIALS
CHARACTERIZATION

Characterization of interfacial reaction products in alumina fiber/barium zirconate coating/alumina matrix composite

Zhongchun Chen, S. Duncan, K.K. Chawla*, M. Koopman, G.M. Janowski

*Department of Materials Science and Engineering, University of Alabama at Birmingham, BEC 254,
1530 3rd Avenue South, Birmingham, AL 35294, USA*

Received 15 December 2001; accepted 15 April 2002

Abstract

Barium zirconate (BaZrO_3) is a candidate material for interface engineering of alumina fiber/alumina matrix composites. Al_2O_3 and BaZrO_3 react at high temperatures to form a series of reaction products. The objective of this work was to characterize these reaction products and to investigate their effect on crack propagation. BaZrO_3 coating was applied on Al_2O_3 fibers via a sol–gel route. The characterization was carried out by X-ray diffraction (XRD), scanning electron microscopy (SEM) and energy dispersive X-ray spectroscopy (EDS). The reaction products between BaZrO_3 coating and Al_2O_3 (fibers and/or matrix) included ZrO_2 , barium monoaluminate ($\text{BaO}\cdot\text{Al}_2\text{O}_3$) and $\text{Ba}\beta\text{-Al}_2\text{O}_3$ ($\text{BaO}\cdot 7.3\text{Al}_2\text{O}_3$). In hot-pressed composites, barium aluminate was mainly present in the form of $\text{Ba}\beta\text{-Al}_2\text{O}_3$. The $\text{Ba}\beta\text{-Al}_2\text{O}_3$ is known to have a layer-type structure, which is likely to be propitious for crack deflection. The interfacial reactions are diffusion-controlled solid-state processes, mainly depending on the diffusion of Ba cations. The $\text{Ba}\beta\text{-Al}_2\text{O}_3$ phase can form either through direct reaction between the BaZrO_3 coating and Al_2O_3 or through indirect reaction between a $\text{BaO}\cdot\text{Al}_2\text{O}_3$ intermediate phase and Al_2O_3 . The BaZrO_3 coating and the reaction products between the coating and fiber/matrix provide multiple weak interfaces, which are likely to result in crack deflection and thus toughness enhancement in an all oxide composite. © 2002 Published by Elsevier Science Inc.

Keywords: Alumina; Barium zirconate; Oxide fiber/oxide matrix composite; Ceramic matrix composite; Interfacial reaction

1. Introduction

Oxide fiber/oxide matrix composites form an important and attractive category of ceramic matrix composites (CMCs) because of their high strength and inherent stability in oxidizing atmospheres at high temperatures [1]. However, such oxide CMCs lack toughness because of strong fiber/matrix inter-

facial bonding. This is a major obstacle to their application at high temperatures.

In order to avoid the chemical interaction between fiber and matrix and form weak fiber/matrix interface (hence improved toughness), incorporation of an interphase(s), i.e., coating of fiber, has been investigated [2–4]. Some stoichiometric oxides, SnO_2 [5–7], LaPO_4 [8–10] and ZrO_2 [11,12], are examples of interphase materials in the $\text{Al}_2\text{O}_3/\text{Al}_2\text{O}_3$ system. These oxide coatings are chemically inert at elevated temperatures with respect to both alumina fiber and alumina matrix. Recently, Gladysz et al. [13] investigated the processing and microstructural devel-

* Corresponding author. Tel.: +1-205-934-8450; fax: +1-205-934-8485.

E-mail address: kchawla@eng.uab.edu (K.K. Chawla).

opment of alumina/barium zirconate (BaZrO_3) laminated composites. In these composites, BaZrO_3 reacts with Al_2O_3 at temperatures around 1475°C to form a series of oxides: ZrO_2 , $\text{BaO}\cdot\text{Al}_2\text{O}_3$ and $\text{BaO}\cdot 6\text{Al}_2\text{O}_3$. Such reactions result in the formation of multiple, weak and stable interfaces. This results in crack deflection, with corresponding potential improvements in fracture toughness. Furthermore, Koopman et al. [14] examined the feasibility of BaZrO_3 as a candidate material for interfacial coating in Al_2O_3 fiber/ Al_2O_3 matrix composites. Unlike common interphase materials, where reactions between interphase and fiber/matrix are not desirable, a BaZrO_3 coating forms multiple interfaces through reactions with Al_2O_3 (both the fiber and matrix) during fabrication of the composites [14]. The purpose of this paper is to investigate the effects of processing parameters on interfacial reaction products and their formation mechanisms.

BaZrO_3 has a cubic perovskite structure and a high melting point of about 2600°C . It is an important technological material and has found widespread applications in dielectrics, piezoelectrics, electrooptic materials, catalysts and proton conductors [15,16]. It was discovered recently that BaZrO_3 does not react with the melt during the crystal growth of high- T_c superconducting compound $\text{YBa}_2\text{Cu}_3\text{O}_{7-\delta}$ [17,18]. BaZrO_3 can be used as an inert crucible material, either as bulk BaZrO_3 crucibles [18] or BaZrO_3 -coated alumina crucibles [19]. Therefore, an examination of the reaction behavior in the $\text{BaZrO}_3/\text{Al}_2\text{O}_3$ system is also significant in regard to the crystal growth of ceramic superconducting materials.

In the present work, interfacial reactions between BaZrO_3 coatings and alumina fibers or matrix during heat treatment and processing of composites have been investigated. The main objective of this research was to identify the reaction products between the BaZrO_3 interphase and Al_2O_3 fiber/matrix and to better understand the mechanisms of formation of the reaction products as well as their effect on crack propagation.

2. Experimental procedure

2.1. Materials

The fiber used in this research was unsized Nextel 610 fiber obtained from 3M (St. Paul, MN). Nextel 610 is a polycrystalline fiber composed of >99 wt.% $\alpha\text{-Al}_2\text{O}_3$ with a diameter of 10–12 μm and 400 filaments per tow. Alumina was also used as a matrix in the composites. The Al_2O_3 powder was 99.99% pure with an average particle size of $\sim 1\ \mu\text{m}$ (Bai-kowski Inter., Charlotte, NC).

2.2. Coating of the fibers

Sol–gel processing was used to prepare a barium zirconate precursor. Barium acetate was dissolved in a continuously stirred mixture of acetic acid and methanol at 70°C , followed by the addition of *n*-propanol ($\text{CH}_3\text{CH}_2\text{CH}_2\text{OH}$) containing 70% *Zr-n*-propoxide ($\text{Zr}[\text{O}(\text{CH}_2)_2\text{CH}_3]_4$). The solution was dried on a hotplate until a dry gel was obtained. The gel was then rehydrated to produce an aqueous solution.

The sol–gel coating of fibers was done with the BaZrO_3 precursor sol. Small pieces of Nextel 610 fabric were injected with BaZrO_3 aqueous sol by means of a syringe. The coated fabric pieces were then dried with a heat gun to produce a dry gel containing Ba, Zr and organic compounds. This was followed by calcining at 800°C for 1 h in air to convert the gel into BaZrO_3 . The coating procedure was repeated a second time to increase thickness of the coating.

2.3. Heat treatment of BaZrO_3 -coated fibers

In order to identify the reactions between BaZrO_3 coating and fibers, the BaZrO_3 coated Nextel 610 fabric samples were heated in the range of $1100\text{--}1500^\circ\text{C}$ in air for 1 h. Additional fabric samples were heat-treated at 1350°C in air for different holding times (1–5 h). The heating rate was $15^\circ\text{C}/\text{min}$ and furnace cooling was used. After heat treatment, the samples were ground into powder by using mortar and pestle for X-ray diffraction (XRD) analysis.

2.4. Preparation of composites

The BaZrO_3 -coated fabrics and alumina powder were arranged in layers within a graphite die and consolidated via uniaxial hot pressing. The fabric planes were perpendicular to the loading direction during hot-pressing. The content of fibers in the composites was 30 vol.%. The hot pressing was performed under vacuum at $1300\text{--}1400^\circ\text{C}$ for 1 h at a pressure of 35 MPa. The heating and cooling rates were 15 and $50^\circ\text{C}/\text{min}$, respectively.

2.5. Characterization

The phase identifications for the samples of BaZrO_3 -coated fibers (in powder form) and hot-pressed composites (in polished pellet form) were carried out by XRD on a Philips MPD 3040 diffractometer with $\text{CuK}\alpha$ radiation and a Ni filter. The parameters for XRD analysis were 45 keV and 40 mA, $0.04^\circ/\text{step}$ and $2.00\ \text{s}/\text{step}$.

Microstructural characterization was performed by scanning electron microscopy (SEM, Philips 515) and energy dispersive X-ray spectroscopy (EDS) was used for compositional analyses. Moreover, the crack propagation paths and the interaction of cracks with the interfaces were examined by SEM observations of the fracture surfaces obtained from three-point bending tests. Samples were sputter coated with Au–Pd prior to examination in the SEM.

3. Results and discussion

3.1. Interfacial reactions between BaZrO₃ coating and Al₂O₃ fibers

The X-ray powder diffraction patterns of BaZrO₃-coated Al₂O₃ fibers that were heat-treated at different temperatures between 1100 and 1500 °C for 1 h are shown in Fig. 1. The XRD pattern consists only of the

peaks of α -Al₂O₃ and BaZrO₃ after heat treatment at 1100 °C (Fig. 1(a)). This indicates that no detectable reactions occur between BaZrO₃ and Al₂O₃ up to 1100 °C in 1 h. At 1200 °C (Fig. 1(b)), in addition to strong peaks of α -Al₂O₃ and BaZrO₃, some small peaks of barium monoaluminate BaAl₂O₄ (BaO·Al₂O₃) and ZrO₂ (monoclinic) phases occur, indicating that BaZrO₃ starts to react with Al₂O₃ to form minor quantities of these phases. It should be noted that the volume of Al₂O₃ in the coated fibers is quite high in relation to the volume of the BaZrO₃ coating. When the temperature is raised to 1300 °C (Fig. 1(c)), the intensity of the peaks of the BaZrO₃ phase is greatly reduced, as the reactions between the coating and fibers proceed. At the same time, the peaks of two reaction products, BaO·Al₂O₃ and ZrO₂, become very strong. At 1400 °C (Fig. 1(d)), however, almost no trace of BaO·Al₂O₃ phase can be found from the XRD pattern, with the dominant phases being barium aluminate Ba_{0.75}Al₁₁O_{17.25} (i.e., BaO·7.3Al₂O₃) and

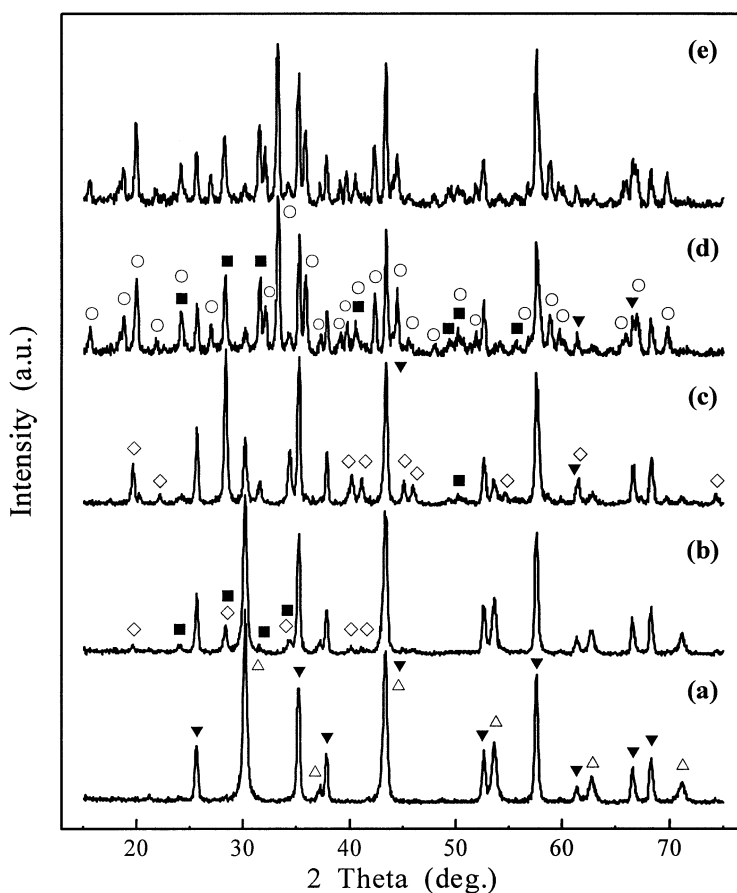


Fig. 1. X-ray powder diffraction patterns of BaZrO₃-coated Al₂O₃ fibers that were heat-treated between 1100 and 1500 °C at intervals of 100 °C for 1 h: (a) 1100 °C, (b) 1200 °C, (c) 1300 °C, (d) 1400 °C and (e) 1500 °C. (Δ) BaZrO₃, (∇) α -Al₂O₃, (\diamond) BaO·Al₂O₃, (\blacksquare) monoclinic ZrO₂ and (\circ) BaO·7.3Al₂O₃.

ZrO₂. Moreover, there exist some small peaks corresponding to BaZrO₃, indicating the presence of remnant BaZrO₃. At 1500 °C, no apparent changes are seen in the pattern (Fig. 1(e)) and the XRD spectrum displays almost the same pattern as that at 1400 °C. It has been shown that barium aluminate, BaO·7.3Al₂O₃, is one of the Ba β-Al₂O₃ compounds (called as β₁ phase) with layered β-Al₂O₃ structure [20,21]. Groppi et al. [20] pointed out that materials with the β-Al₂O₃ structure could be obtained in the range of 9.1–14.6 of the Al/Ba ratio.

The above results show that the barium aluminates produced through reactions between BaZrO₃ and Al₂O₃ are different after one hour at 1300 °C and after 1 h at 1400 °C. At 1300 °C, the BaO·Al₂O₃ phase occurs, while at 1400 °C and above, the BaO·7.3Al₂O₃ phase is obtained. This is to say, a Ba-rich phase occurs at lower temperature and an Al-rich phase forms at higher temperature. In general, in an oxide/oxide system, reactions occur by diffusion of ions from an oxide with lower bond energy to another oxide with higher bond energy. According to the thermodynamic data in Ref. [22], the bond energies of BaO and Al₂O₃ at 0 K are 574 and 2211 kJ/mol, respectively. It is consequently believed that the reactions between BaZrO₃ and Al₂O₃ are diffusion-controlled solid-state processes, and the diffusion of Ba cations dominates the reaction process in the BaZrO₃/Al₂O₃ system. In this way, at higher temperatures, long-distance dif-

fusion of Ba results in the formation of a Ba-poor and, thus, Al-rich phase.

The XRD results of BaZrO₃-coated Al₂O₃ fibers after heat treatment at 1350 °C for different holding times (1, 2 and 5 h) are shown in Fig. 2. For the pattern of 1 h (Fig. 2(a)), the BaO·Al₂O₃ phase still has high relative intensity, although it is somewhat weaker compared to the XRD pattern of 1300 °C (Fig. 1(c)). Of significance is that the BaO·7.3Al₂O₃ phase starts to form. With the increase in time, the relative intensity of the peaks of the BaO·Al₂O₃ phase gradually decreases and some weak peaks disappear. On the other hand, the BaO·7.3Al₂O₃ phase exhibits stronger diffraction peaks with the increase of reaction product. This suggests that BaO·Al₂O₃ is an intermediate phase. The BaO·7.3Al₂O₃ phase can be formed through the consumption of BaO·Al₂O₃ phase, that is, by further reaction between BaO·Al₂O₃ and Al₂O₃. When the holding time reaches 5 h (Fig. 2(c)), the XRD pattern is almost the same as that at 1400 and 1500 °C for 1 h (Fig. 1(d) and (e)). These results indicate that an increase of holding time has an effect similar to the increase in heat-treatment temperature.

3.2. Interfacial reactions in BaZrO₃-coated Al₂O₃ fiber/Al₂O₃ matrix composites

The XRD patterns of BaZrO₃-coated Al₂O₃ fiber/Al₂O₃ matrix composites obtained via hot-pre-

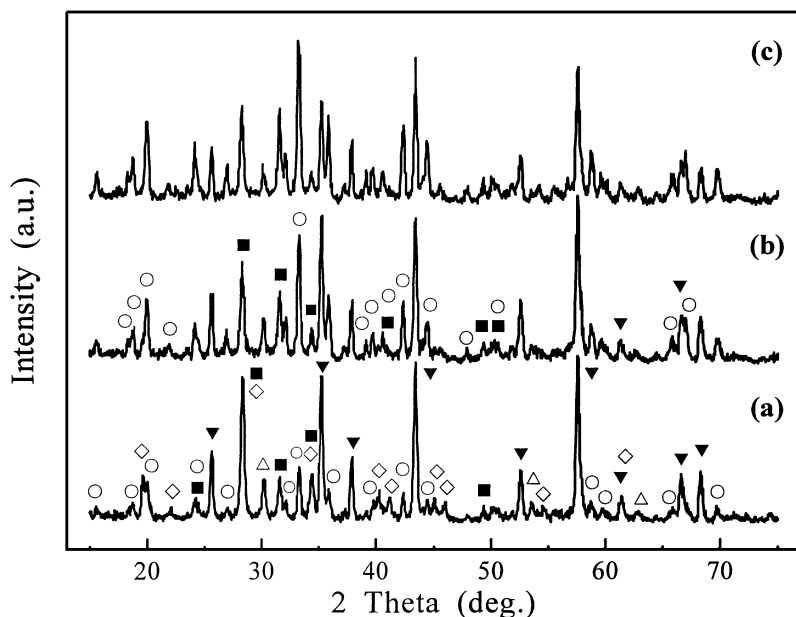


Fig. 2. X-ray powder diffraction patterns of BaZrO₃-coated Al₂O₃ fibers obtained from heat treatment at 1350 °C for different holding times: (a) 1 h, (b) 2 h and (c) 5 h. (Δ) BaZrO₃, (▼) α-Al₂O₃, (◇) BaO·Al₂O₃, (■) monoclinic ZrO₂ and (○) BaO·7.3Al₂O₃.

ssing at 1300 and 1400 °C are shown in Fig. 3. Both X-ray spectra are very similar to each other. Although the peaks of reaction products are very weak because of the small amount of reaction products in the Al₂O₃ fiber/Al₂O₃ matrix composites (excess of Al₂O₃), one can note the presence of the peaks of BaO·7.3Al₂O₃ and ZrO₂ phases, in addition to small peaks of unreacted BaZrO₃ coating and strong Al₂O₃ peaks. As for the XRD pattern of the composite hot-pressed at 1300 °C (Fig. 3(a)), it exhibits a different pattern from that of BaZrO₃-coated fiber heat-treated at the same temperature (Fig. 1(c)). The difference lies in Al/Ba atomic ratio in reaction products (barium aluminate). In the composite hot-pressed at 1300 °C, it corresponds to the ratio of Al/Ba=14.6 (BaO·7.3 Al₂O₃) with β-Al₂O₃ structure, while in BaZrO₃ coated fiber heat-treated at the same temperature, it corresponds to the ratio of Al/Ba=2 (BaO·Al₂O₃). We estimate that the Al-rich BaO·7.3Al₂O₃ phase has a density value of ~3.6 g cm⁻³ (less than that of α-Al₂O₃) [23]. It seems reasonable to point out that the density of Ba-rich BaO·Al₂O₃ phase has a density less than that of BaO·7.3Al₂O₃. This reasoning suggests that the pressure during hot-pressing of composites promotes the formation of barium aluminates with high Al/Ba atomic ratio (Al₂O₃-rich phase). Even though BaO·7.3Al₂O₃ phase may be formed at higher temperatures or longer holding times without the application of pressure (see Figs. 1 and 2), the intimate contact between BaZrO₃ coating and alumina fibers/matrix under the pressure speeds up the reaction process.

3.3. Effect of interfacial reactions on microstructure and crack propagation

A typical backscattered electron image of a polished cross-section (perpendicular to the fabric plane) of a hot-pressed alumina fiber/alumina matrix composite is shown in Fig. 4. In this micrograph, there exist white, light gray and dark gray regions. The contrast in this micrograph is mainly associated with the mean atomic number of each region. Bright regions correspond to high atomic numbers (Zr and Ba in this case), and dark features correspond to low atomic number (Al). The spectra for positions marked by numbers in the micrograph are also given in Fig. 4. For positions 1 and 5, which correspond to the Al₂O₃ matrix and the central region of an Al₂O₃ fiber, respectively, the spectra show the presence of Al and O, as expected. Note that two small peaks in the range of 2–3 keV in EDS spectra shown in Fig. 4 come from the Au–Pd sputter coating. For positions 2 and 6, there are small Ba peaks and large Al peaks, attributed to Ba β-Al₂O₃ in the surface region of a fiber (6) and in the matrix adjacent to a fiber (2), because of the reaction between the BaZrO₃ coating and alumina fibers or matrix. In interfacial regions between adjacent fibers (positions 3 and 4), intense Zr peaks indicate the presence of ZrO₂. It is shown that the ZrO₂ phase forms at those positions where the BaZrO₃ coating was originally present (i.e., surfaces of fibers or interfacial regions between adjacent fibers).

From the above results, it can be concluded that the white, light gray and dark gray regions shown in Fig. 4 correspond to ZrO₂, Ba β-Al₂O₃ and Al₂O₃

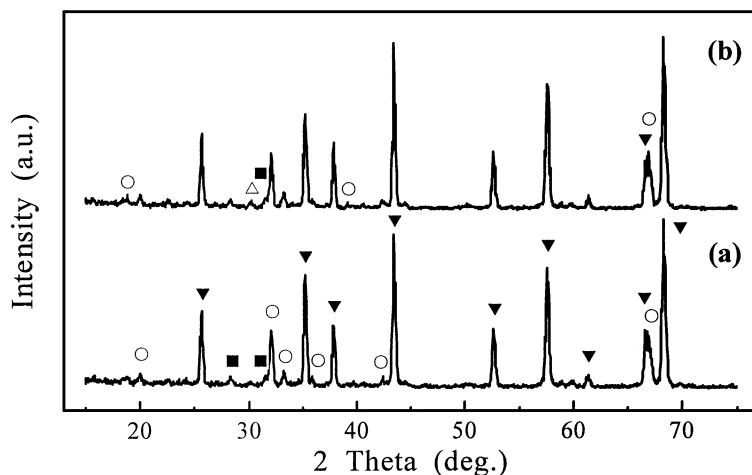


Fig. 3. XRD patterns of BaZrO₃-coated Al₂O₃ fiber/Al₂O₃ matrix composites after hot-pressing at (a) 1300 °C and (b) 1400 °C, respectively. (△) BaZrO₃, (▼) α-Al₂O₃, (◇) BaO·Al₂O₃, (■) monoclinic ZrO₂ and (○) BaO·7.3Al₂O₃.

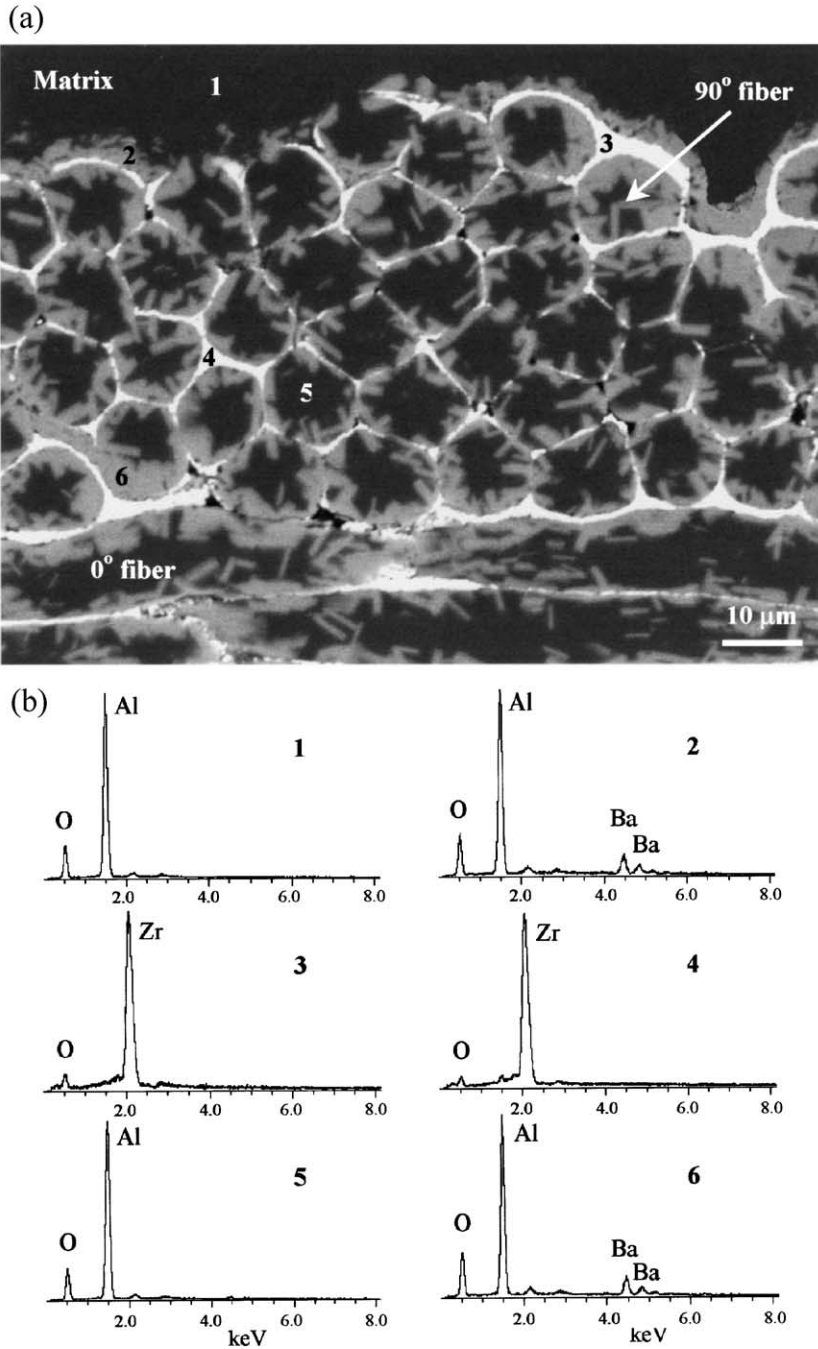


Fig. 4. (a) SEM micrograph showing the microstructure of a polished cross-section of an alumina fiber/alumina matrix composite (backscattered electron mode, 18 kV). (b) EDS spectra were taken in regions indicated by numbers.

phases, respectively. It is noted that the presence of a BaZrO₃ coating impedes the fiber/fiber bonding and fiber/matrix bonding. The interfacial reaction products (such as ZrO₂ and Ba β-Al₂O₃) between BaZrO₃ coating and alumina fibers or alumina matrix are likely to provide weak interfaces in the composites.

An SEM micrograph (Fig. 5) shows the crack propagation path in a composite during three-point bending test, which illustrates the effect of these interfacial reaction products. The crack, which formed during the bending test, propagated along the 0/90° interface of the Nextel 610 fabric. The Zr-

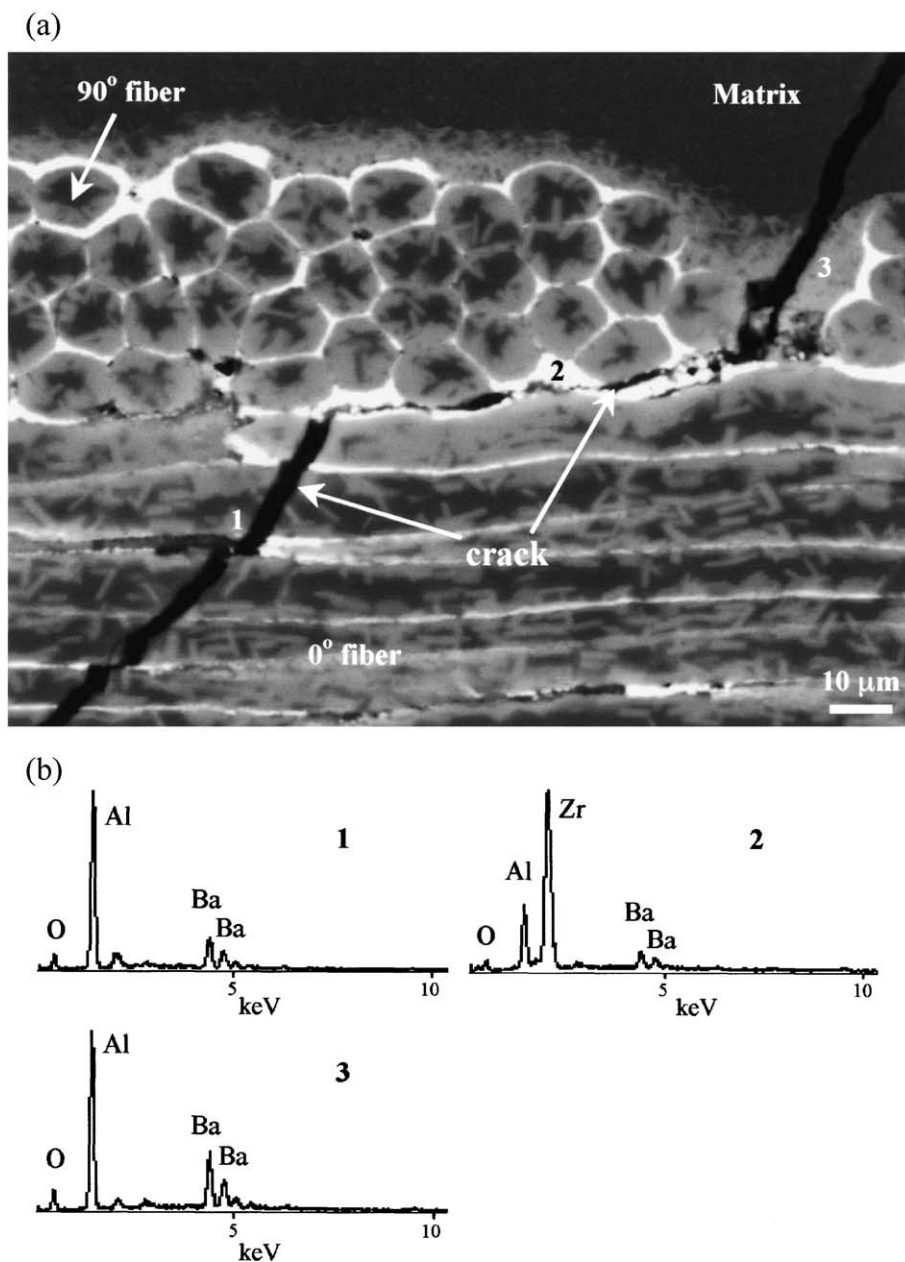


Fig. 5. (a) SEM micrograph showing crack propagation through an alumina fiber/alumina matrix composite (backscattered electron mode), cracked via a three-point bending test. (b) EDS spectra were taken in regions indicated by numbers.

rich region near the 0/90° interface (see EDS pattern of position 2 in Fig. 5) may be attributed to ZrO_2 and small amount of $BaZrO_3$, which remained after processing. This indicates that the interfaces of both ZrO_2 and $BaZrO_3$ phases with alumina fibers are significantly weak and contribute to a damage tolerant behavior in these composites. It can be seen from the micrographs (Figs. 4 and 5) that there is a larger thickness of coating at the 0/90° interface and

at the surface of fabric, compared to those fibers located in the interior region of a tow. This is understandable because the distance between adjacent fibers determines the coating thickness. For those fibers inside a tow, a small distance causes a thin coating. At the 0/90° interface, there is a larger interfiber distance; and of course, during the sol–gel coating process, the surface of a fabric is free, thus a thick coating is easily formed.

In addition to ZrO_2 and $BaZrO_3$ interfaces, other interfaces, formed through reactions between the $BaZrO_3$ coating and alumina (fibers and matrix), can also influence the crack propagation. As seen in Fig. 5, the crack crosses through the 0° fibers (lower left) and matrix (upper right). From the EDS spectra from positions 1 and 3 (Fig. 5) surrounding the crack, it is seen that these regions have more Al and Ba, suggesting the presence of $Ba \beta-Al_2O_3$ phases, even though there is a difference in Ba content between positions 1 and 3. Consequently, the interface of $Ba \beta-Al_2O_3$ with alumina fibers or alumina matrix is another source of weak interface. Furthermore, it has been found that $Ba \beta-Al_2O_3$ phase has an anisotropic layered oxide structure [24,25]. These layered oxides themselves are capable of easy cleavage along basal planes, thus, improving the fracture toughness of composites.

In regard to the formation of the ZrO_2 phase, it can result from degradation of $BaZrO_3$, i.e., the diffusion of Ba from the $BaZrO_3$ coating. Another possibility is that the high BaO partial pressure at elevated temperatures [26] leads to evaporation of BaO during the hot-pressing and ZrO_2 phase formation. A schematic view of the formation of reaction products between $BaZrO_3$ coating and an Al_2O_3 fiber is shown in Fig. 6. Whether $BaZrO_3$ coating remains after heat treatment or hot-pressing depends on the coating thickness, temperature, time and pressure. The diffusion of Ba cations and/or evaporation of BaO lead to the formation of the ZrO_2 phase in the location of $BaZrO_3$ coating. It should be noted that the ZrO_2 phase has a monoclinic structure in this work (see Figs. 1 and 2), which is a result of the transformation of ZrO_2 from the tetragonal structure during cooling.

Concurrent with the formation of ZrO_2 , the diffusion of Ba cations to Al_2O_3 gives rise to the formation of barium aluminates $BaO \cdot xAl_2O_3$ around the Al_2O_3 fiber (x : half of Al/Ba ratio). The value of x is determined by processing parameters. At lower temperature, for example, below $1300^\circ C$ for 1 h, $x = 1$, that is, $BaO \cdot Al_2O_3$ forms as shown in Fig. 1. As the reaction proceeds, the reaction products are predominantly $Ba \beta-Al_2O_3$. As mentioned in the previous section, $Ba \beta-Al_2O_3$ phase can be formed through the reaction between $BaO \cdot Al_2O_3$ and Al_2O_3 . Another possible mechanism is the direct reaction between the $BaZrO_3$ coating and Al_2O_3 with the help of the diffusion of Ba cations. Groppi et al. [20] showed the formation of $Ba \beta-Al_2O_3$ phase by solid-state reaction between $\gamma-Al_2O_3$ and dispersed barium. Of $Ba \beta-Al_2O_3$ compounds, those with Al/Ba = 13.8–15.4 ($x = 6.9$ –7.7 in $BaO \cdot xAl_2O_3$) seem to have nearly the same peak positions in JCPDS data. Although the results of XRD and EDS analyses in this investigation indicate the presence of $Ba \beta-Al_2O_3$ phases, actually there exist differences in Ba content, as shown in Figs. 4 and 5. Therefore, in the region marked $BaO \cdot xAl_2O_3$ in Fig. 6, the value of x does not remain constant, because of the existence of a concentration gradient of Ba during diffusion. Gladysz et al. [13] found the presence of $BaO \cdot 6Al_2O_3$ phase via electron diffraction in a small area of laminated composites of $Al_2O_3/BaZrO_3$. Their reported value of x is smaller than that reported in this work. From the above discussion, it is believed that the occurrence of the $BaO \cdot 6Al_2O_3$ phase is possible in some small region of reaction. Furthermore, they observed that the reaction products were arranged in a sequence, which is in good agreement with the formation mechanism of reaction products proposed in Fig. 6.

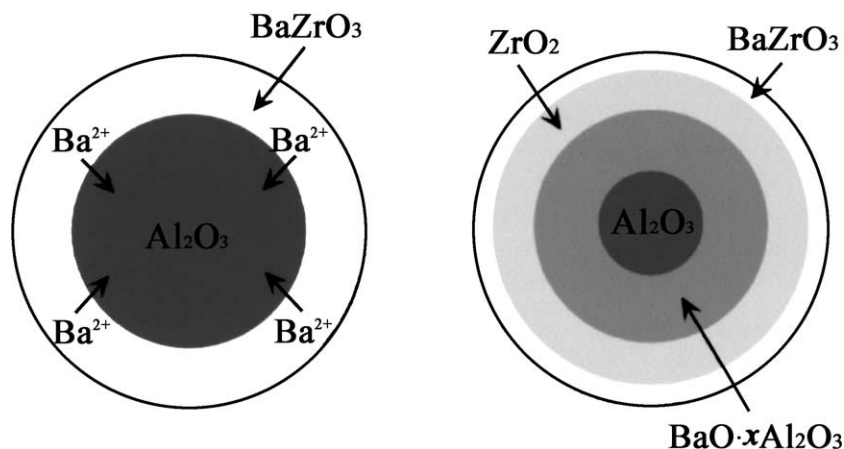


Fig. 6. Schematic illustration of the formation of reaction products between $BaZrO_3$ coating and an Al_2O_3 fiber in the range of 1200 – $1500^\circ C$. The diffusion of Ba cations controls the reaction process.

4. Conclusions

Alumina matrix or fiber reacts with the barium zirconate coating produced via a sol–gel technique during heat treatment or processing of composites above 1200 °C for 1 h. The reaction products include ZrO_2 , barium monoaluminate ($BaO \cdot Al_2O_3$) and $Ba \beta-Al_2O_3$ ($BaO \cdot 7.3Al_2O_3$). In composites hot-pressed above 1300 °C (1 h), barium aluminate is mainly present in the form of $Ba \beta-Al_2O_3$. The reactions between the $BaZrO_3$ coating and alumina fiber/matrix are diffusion-controlled solid-state processes, mainly depending on the diffusion of Ba cations. $Ba \beta-Al_2O_3$ phase can be formed either through direct reaction between the $BaZrO_3$ coating and Al_2O_3 or through indirect reaction between the $BaO \cdot Al_2O_3$ intermediate phase and Al_2O_3 . The application of pressure during hot-pressing of the composites is likely to promote formation of $Ba \beta-Al_2O_3$ by increasing the degree of contact between the $BaZrO_3$ coating and the fiber/matrix. The $BaZrO_3$ coating and the reaction products between the coating and alumina (fibers and matrix), such as ZrO_2 and $Ba \beta-Al_2O_3$, provide multiple weak interfaces in the composites and are propitious for crack deflection at interfaces.

Acknowledgements

The authors acknowledge gratefully the financial support for this work from the U.S. Office of Naval Research (Contract #N00014-99-1-0909). Dr. A.K. Vasudevan and Dr. S.G. Fishman were the program managers. They also wish to express their gratitude to 3M for providing Nextel 610 fabric.

References

- [1] Chawla KK, Coffin C, Xu ZR. Interface engineering in oxide fiber/oxide matrix composites. *Int Mater Rev* 2000;45:165–89.
- [2] Chawla KK. Ceramic matrix composites. London: Chapman and Hall, 1993.
- [3] Faber KT. Ceramic composite interfaces: properties and design. *Annu Rev Mater Sci* 1997;27:499–524.
- [4] Kim JK, Mai YW. Engineered interfaces in fiber reinforced composites. New York: Elsevier, 1998.
- [5] Chawla KK, Xu ZR, Venkatesh R, Ha JS. Interface engineering in some oxide/oxide composites. *ICCM 9*, Madrid, Spain. 1994. p.788–95.
- [6] Siadati MH, Chawla KK, Ferber M. The role of the SnO_2 interphase in an alumina/glass composite: a fractographic study. *J Mater Sci* 1991;26:2743–9.
- [7] Lundberg R, Pejryd L, Butler E, Ekelund M, Nygren M. Development of oxide composites. In: Naslain R, Lamont J, Doumeings D, editors. *Proc. Int. Conf. High Temperature Ceramic Matrix Composites I*. UK: Woodhead Publ., 1993. p. 167–74.
- [8] Morgan PED, Marshall DB. Ceramic composites of monazite and alumina. *J Am Ceram Soc* 1995;78:1553–63.
- [9] Kuo D-H, Kriven WM, Mackin TJ. Control of interfacial properties through fiber coatings: monazite coating in oxide–oxide composites. *J Am Ceram Soc* 1997;80:2987–96.
- [10] Chawla KK, Liu H, Janczak-Rausch J, Sambasivan S. Microstructure and properties of monazite ($LaPO_4$) coated saphikon fiber/alumina matrix composites. *J Eur Ceram Soc* 2000;20:551–9.
- [11] Davis JB, Loefvander JPA, Evans AG, Bischoff E, Emiliani ML. Fiber coating concepts for brittle-matrix composites. *J Am Ceram Soc* 1993;76:1249–57.
- [12] Lewis MH, Cain MG, Doleman P, Razzell AG, Gent J. Development of interfaces in oxide and silicate matrix composites. In: Evans AG, Naslain R, editors. *High-temperature ceramic-matrix composites II*. Westerville, OH: American Ceramic Society, 1995. p. 41–52.
- [13] Gladysz GM, Schmuecker M, Chawla KK, Schneider H, Joslin DL, Ferber MK. Characterization of the reaction products that develop in the processing of $Al_2O_3/BaZrO_3$ laminated compounds. *Mater Charact* 1998;40:209–14.
- [14] Koopman M, Duncan S, Chawla KK, Coffin C. Processing and characterization of barium zirconate coated alumina fiber/alumina matrix composites. *Compos, Part A* 2001;32:1039–44.
- [15] Kingery WD, Bowen HK, Uhlmann DR. *Introduction to ceramics*. New York: Wiley, 1976.
- [16] Iwahara H, Yajima T, Hibino T, Ozaki K, Suzuki H. Protonic conduction in calcium, strontium and barium zirconates. *Solid State Ionics* 1993;61:65–9.
- [17] Erb A, Walker E, Flukiger R. $BaZrO_3$: the solution for the crucible corrosion problem during the single crystal growth of high- T_c superconductors $REBa_2Cu_3O_{7-\delta}$; RE = Y, Pr. *Physica C* 1995;245:245–51.
- [18] Erb A, Walker E, Flukiger R. The use of $BaZrO_3$ crucibles in crystal growth of the high- T_c superconductors: progress in crystal growth as well as in sample quality. *Physica C* 1996;258:9–20.
- [19] Shi J, Berger JE, Ling XS. Growth of $YBa_2Cu_3O_7$ -crystals with $BaZrO_3$ -coated alumina crucibles. *Physica C* 1998;301:215–20.
- [20] Groppi G, Cristiani C, Forzatti P. Phase composition and mechanism of formation of $Ba\beta$ -alumina-type systems of catalytic combustion prepared by precipitation. *J Mater Sci* 1994;29:3441–50.
- [21] Dunn S, Kumar RV, Fray DJ. Thermodynamic studies of the ionic conductor $\beta-Al_2O_3$. *Solid State Ionics* 2000;128:141–4.
- [22] Vedenyev VI, Gurchik LV, Kondrat'yev VN, Medvedev VA, Frankeich YeL. Bond energies, ionization potentials and electron affinities. New York: St Martin's Press, 1966 (Translated from the Russian by Scripta Technica).
- [23] Chen ZC, Chawla KK, Koopman M. Microstructure and mechanical properties of in-situ synthesized alu-

- mina + barium- β -alumina + zirconia composites, to be published.
- [24] van Berkel FPF, Zandbergen HW, Verschoor GC, Ijdo DJW. The structure of barium aluminate, $\text{Ba}_{0.75}\text{Al}_{11}\text{O}_{17.25}$. *Acta Crystallogr* 1984;C40:1124–7.
- [25] Cinibulk MK, Hay RS. Textured magnetoplumbite fiber-matrix interphase derived from sol–gel fiber coating. *J Am Ceram Soc* 1996;79:1233–46.
- [26] Odoj R, Hilpert K. Evaporation and standard enthalpy of formation of $\text{BaZrO}_3(\text{s})$. *Z Phys Chem (NF)* 1976; 102:191–201.